British Journal of Dermatology Advance access publication date: 19 April 2025 **Translational Research**

Genetic and environmental factors affecting hair density in East Asian populations

Qili Qian[®], Yuanping Gu, Junyu Luo, 1,2 Sijie Wu, Jiapeng Li, Jinxi Li, Qianqian Peng, 1 Wenyan Chen,¹ Yajun Yang,^{4,5} Jiucun Wang⁰,³ Li Jin,³ Renliang Sun,¹ Guoqing Zhang,^{1,5} Fan Liu^{©6} and Sijia Wang^{©1}

CAS Key Laboratory of Computational Biology, Shanghai Institute of Nutrition and Health, University of Chinese Academy of Sciences, Chinese Academy of Sciences, Beijing, China

²Guangzhou National Laboratory, Guangzhou International Bio Island, Guangzhou, China

³State Key Laboratory of Genetic Engineering, Human Phenome Institute, Zhangjiang Fudan International Innovation Center, Fudan University, Shanghai, China

⁴Ministry of Education Key Laboratory of Contemporary Anthropology, Collaborative Innovation Center for Genetics and Development, School of Life Sciences, Fudan University, Shanghai, China

⁵Fudan-Taizhou Institute of Health Sciences, Taizhou, China

Department of Forensic Sciences, College of Criminal Justice, Naif Arab University for Security Sciences, Riyadh, Saudi Arabia

Correspondence: Sijia Wang. Email: wangsijia@sinh.ac.cn

Q. Qian, Y. Gu and J. Luo contributed equally to this work.

F. Liu and S. Wang jointly supervised this work.

Abstract

Background Hair density traits, including follicular unit density (FUD) and hairs per follicular unit (HFU), are influenced by environmental and genetic factors. Understanding these determinants can refine our knowledge of hair growth patterns and enable more targeted interventions. Historically, large-scale research has been constrained by difficulties in precise phenotyping.

Objectives To identify environmental and genetic factors associated with hair density in East Asian populations and to explore shared genetic influences among other hair traits and hair disorders.

Methods We performed quantitative assessments of FUD and HFU using trichoscopic images from 5735 East Asian individuals. Accurate phenotyping was achieved through deep learning-based analyses with manual correction. We used multiple regression to evaluate demographic, lifestyle and reproductive factors, and conducted genome-wide association studies (GWAS), meta-analysis and a combined GWAS (C-GWAS) for hair density, hair curliness, eyebrow thickness and beard thickness. Significant associations were compared with published results on male pattern baldness (MPB). Gene-finasteride use interactions were evaluated via mixed linear models in longitudinal UK Biobank

Results Age, sex, body mass index and menopausal status were significantly associated with FUD and HFU. Three genetic loci, rs11940736 at 4q28.1 (near SPRY1), rs10908366 at 1p34.3 (near RSPO1) and rs3771033 at 2q23.3 (intron NRP2), showed significant associations with hair density, with functional annotations implicating these genes in hair follicle development. In particular, rs3771033 was a significant expression quantitative trait locus for NRP2, where the T allele correlated with lower NRP2 expression but higher FUD. We also found substantial genetic overlap among hair density traits, hair curliness, eyebrow thickness, beard thickness and MPB. In UK Biobank analyses, rs3771033 exhibited allele-specific treatment effects on finasteride response in MPB.

Conclusions We identified three loci that shape hair density in East Asian populations. Our results clarify the genetic and environmental architecture underlying hair density traits and suggest that genotype-specific responses to finasteride may open new avenues for the personalized management of hair disorders.

Lay summary

Hair loss is caused by common conditions such as male pattern baldness. The condition affects millions of people worldwide and can have an impact on a person's confidence and quality of life.

This study was carried out by researchers in China, to try to understand the causes of differences in hair density in East Asian people. We aimed to identify genetic and environmental factors that determine how thick or full a person's hair appears.

Using advanced genetic techniques, we examined the DNA from 5735 Chinese Han participants. We also assessed hair density through detailed imaging techniques. We also considered other factors like age, sex, BMI ('body mass index') and menopausal status. We found that three important genes were linked to hair density. These genes are called 'SPRY1', 'RSPO1' and 'NRP2'. They were also associated with hair loss conditions like male pattern baldness. We also found that people with certain genetic variations respond differently to a common hair loss medication called 'finasteride'. This suggests that treatments could be personalized based on a person's genetics.

Our findings offer hope for more effective, tailored, hair loss treatments in the future. Understanding the genetic factors involved in hair density could lead to new therapies. This study also highlights how important genetics and lifestyle are in managing hair health. Future research should explore these genetic links further. It should also test personalized treatment approaches to improve outcomes for people experiencing hair loss.

What is already known about this topic?

- Hair density, determined by follicular unit density and hairs per follicular unit, varies across individuals and ethnic groups, indicating a strong genetic component.
- · Variations in hair density have clinical relevance, serving as diagnostic markers in conditions like baldness.
- The genetic and environmental determinants of hair density remain underexplored, mainly due to challenges in accurate phenotyping.

What does this study add?

- A cohort of 5735 Chinese Han participants clarifies key environmental factors that influence hair density.
- Three newly identified genetic loci (SPRY1, RSPO1, NRP2) modulate hair density traits, with functional links to hair follicle development.
- There is substantial genetic overlap among hair density traits, hair curliness, eyebrow thickness, beard thickness and male pattern baldness (MPB), along with evidence of genotype-specific responses to finasteride in MPB.

What is the translational message?

- Identification of SPRY1, RSPO1 and NRP2 provides potential targets for hair regeneration therapies.
- Insights into the shared genetic foundations of related traits and disorders may facilitate the development of treatments that address multiple conditions simultaneously.
- · Genotype-specific finasteride responses open avenues for personalized treatment in hair loss management.

Hair density, defined by the number of hair follicles per unit scalp area [follicular unit density (FUD)] and the number of hair strands per follicular unit [hairs per follicular unit (HFU)], plays a pivotal role in determining perceived hair thickness and fullness. This trait varies substantially among individuals and across ethnic groups, indicating a strong genetic influence.^{1–5} Moreover, variations in hair density can serve as early clinical markers of conditions such as baldness, nutritional deficiencies and hormonal imbalances, ^{6–8} emphasizing its clinical significance.

Descriptive studies indicate that FUD tends to be highest among White populations, followed by East Asian and African populations, ^{1,4} whereas HFU displays an inverse pattern, with African populations generally exhibiting more hairs per follicular unit than White and East Asian populations. ^{3–5} While other hair-related traits such as hair curliness,

eyebrow thickness, beard thickness and male pattern baldness (MPB) have been extensively studied via large-scale genome-wide association studies (GWAS), 9-15 the genetic foundations of hair density remain comparatively understudied. This knowledge gap largely stems from the challenging phenotyping protocols, which often involve shaving regions of the scalp (an aesthetic barrier to participant recruitment), and the labour-intensive nature of accurately quantifying the phenotype.

In this study, we conducted quantitative assessments of FUD and HFU using trichoscopic images from a large cohort of East Asian individuals of Chinese Han descent, focusing on the occipital scalp, an area largely unaffected by androgen-driven hair loss. 16,17 By performing GWAS on these data and integrating the results with existing findings on hair curliness, eyebrow thickness, beard thickness and MPB, we

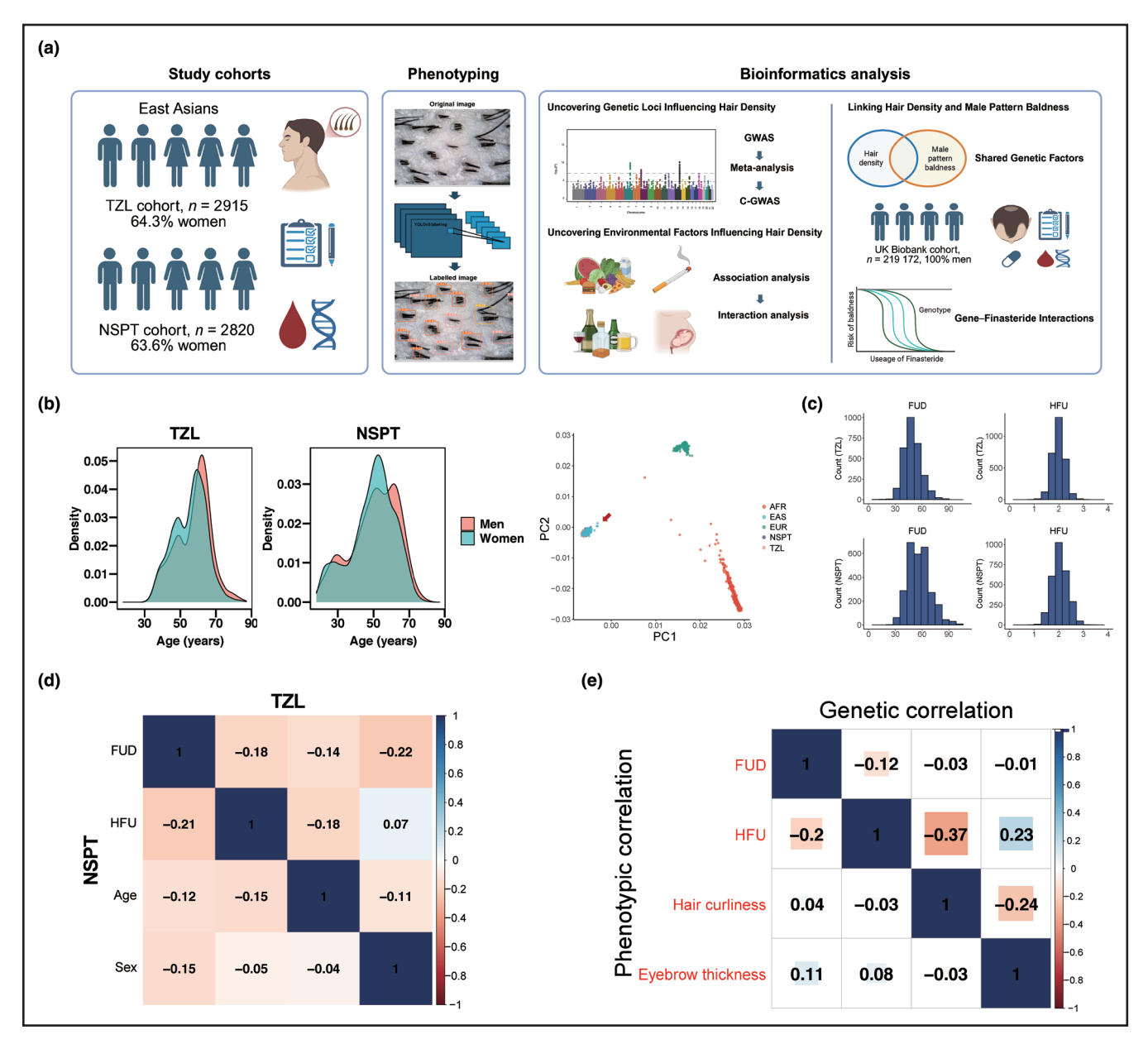


Figure 1 Descriptive statistics and population structure for hair density traits in the Taizhou Longitudinal Study (TZL) and National Survey of Physical Traits (NSPT) cohorts. (a) Schematic of study design and computational analyses. (b) Density plots of age distribution stratified by sex in the TZL and NSPT cohorts (left panel). Principal component (PC) analysis plot (right panel) showed genetic similarity between the TZL and NSPT cohorts (blue and green, respectively) compared with global populations from the 1000 Genomes Project. (c) Phenotypic distributions of follicular unit density (FUD) and hairs per follicular unit (HFU) in the TZL and NSPT cohorts. (d) Phenotypic correlations between FUD, HFU, age and sex in the TZL and NSPT cohorts. (e) Genetic and phenotypic correlations among hair-related traits, including FUD, HFU, hair curliness and eyebrow thickness. AFR, African; C-GWAS, combined GWAS; EAS, East Asian; EUR, European; GWAS, genome-wide association studies. Graphical illustration was created in BioRender. Peng, Q. (2025) https://BioRender.com/bpm1lz1.

aimed to elucidate the shared genetic and environmental underpinnings of these hair-related phenotypes.

Materials and methods

Study participants

After all quality control procedures, 5735 individuals were included in this study. The discovery dataset included 2915 participants [mean (SD) age 56.2 (9.5) years, 64.3% women (n=1875/2915)] from the Taizhou Longitudinal Study (TZL)

cohort.¹⁸ The replication dataset comprised 2820 individuals [mean (SD) age 49.9 (12.8) years, 63.6% women (n=1794/2820)] from the National Survey of Physical Traits (NSPT) cohort [Figure 1; Table S1 (see Supporting Information)].¹⁹

Trichoscopy image analysis and phenotype quantification

Trichoscopy images were captured from the occipital region of the scalp, covering approximately 0.63 cm². FUD and HFU were primarily quantified manually, with deep learning

models assisting in expediting the process, followed by manual review and correction to ensure precision.

Full details of the methods used for phenotyping, quality control, descriptive statistics, GWAS, meta-analysis, replication analysis, combined GWAS (C-GWAS), functional annotations, longitudinal analysis and other statistical analysis are provided in Appendix S1 (see Supporting Information).

Results

Phenotyping, sample characteristics and environmental factors

Hair density phenotypes followed normal distributions in both cohorts [mean (SD) FUD 49.9 (9.6) follicular units (FU) cm⁻² in TZL, and 56.6 (9.6) FU cm⁻² in NSPT; mean (SD) HFU 1.99 (0.25) hairs per FU in TZL and 2.05 (0.32) hairs per FU in NSPT] [Figure 1; Table S2 (see Supporting Information)]. FUD was significantly negatively correlated with HFU (P=1.46×10⁻³²), meaning that for each additional HFU, FUD decreased by an average of 6.34 cm⁻². Every 10-year increase in age resulted in a significant reduction of 1.95 cm⁻² in FUD (P=2.03×10⁻⁵⁰) and a reduction of 0.05 in HFU (P=6.83×10⁻⁴⁵; Table S2). Men exhibited significantly higher FUD than women (mean difference 4.19 cm⁻²; P=1.39×10⁻³⁹) in both cohorts, while the impact of sex on HFU was minimal (P=3.64×10⁻³).

Table S1 details the distribution of 17 demographic, lifestyle and reproductive factors that were tested for association with hair density using multiple regression (Table S3; see Supporting Information). Body mass index (BMI) had a negative association with FUD ($P=2.98\times10^{-6}$), with every 10-unit increase in BMI corresponding to a 2.0 cm⁻² decrease in FUD and a positive association with HFU ($P=9.05\times10^{-5}$), corresponding to an increase of 0.1 hairs

per follicle. Menopausal status was correlated with lower FUD ($P=1.06\times10^{-3}$). Conversely, earlier age at menarche had a positive association with HFU ($P=2.00\times10^{-5}$), while an older age at first pregnancy was associated with lower HFU ($P=1.04\times10^{-3}$). These findings align with previous reports on the influence of BMI and menopause on the risk of hair loss. ^{20–22} Furthermore, we found no credible evidence to support the effect of smoking, alcohol consumption or nutrition on hair density.

Using longitudinal data from the UK Biobank (n=219 172, followed for 13 years), survival analysis using a Cox model confirmed that BMI had a highly significant yet marginal effect on the risk of MPB (hazard ratio 1.09 per 10-unit increase in BMI; P=1.98×10⁻⁶). Thus, it is plausible that the effect of BMI on MPB may stem from its impact on FUD and HFU.

Genome-wide association studies identified three hair density-associated loci

Genomic principal component analysis combining our study cohorts with reference data from the 1000 Genomes Project (1000GP) confirmed that our participants grouped closely with East Asian populations (Figure 1). Heritability estimates (h2) obtained using genome-wide complex trait analysis were substantial, at 0.42 (SE 0.04) for FUD and 0.30 (SE 0.05) for HFU. In the TZL cohort, additional phenotypic measures of hair curliness and evebrow thickness were available from previously reported GWAS, 12,23 allowing us to calculate phenotypic and genetic correlations among FUD, HFU, hair curliness and eyebrow thickness (Figure 1). Notably, the genetic correlations were consistently stronger than the phenotypic correlations, exemplified by a genetic correlation of 0.23 between HFU and eyebrow thickness vs. a phenotypic correlation of 0.08, indicating that environmental factors may contribute considerably to the observed

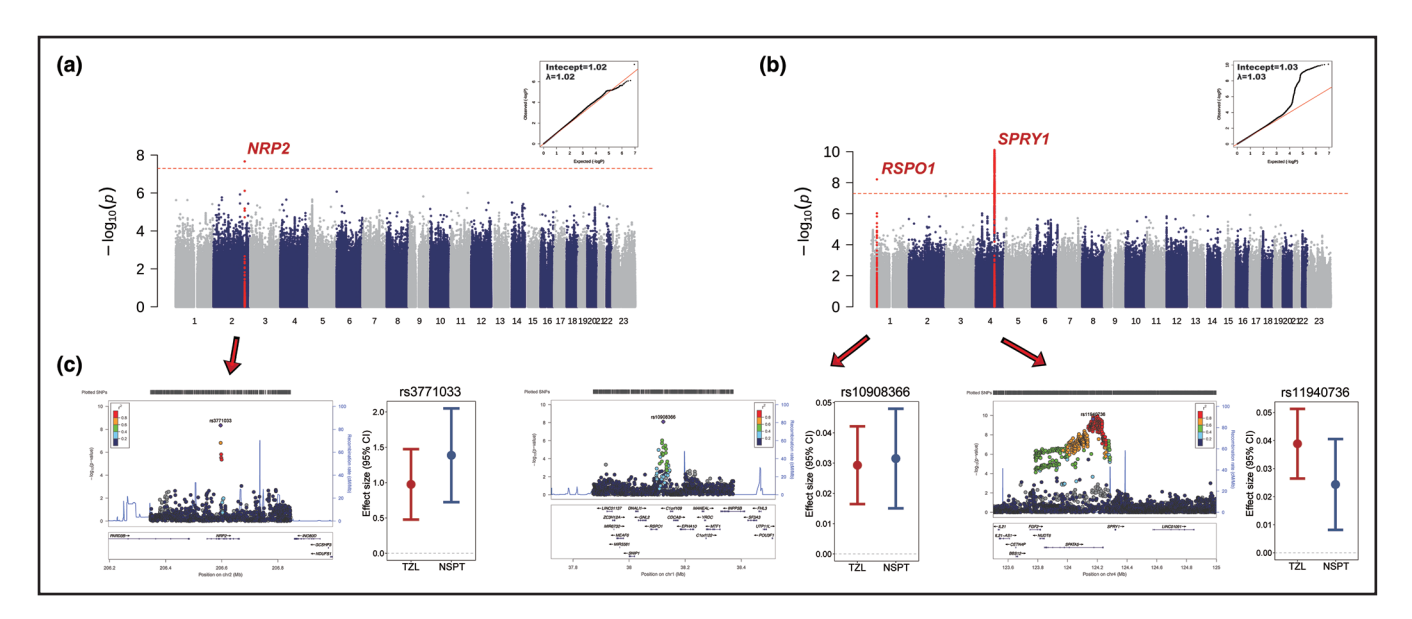


Figure 2 Meta-analysis of hair density identified novel signals in East Asian populations. Manhattan plot and quantile—quantile plot of the meta-analysis result for (a) follicular unit density (FUD) and (b) hairs per follicular unit (HFU). (c) Regional association plots for the identified loci from left to right: rs3771033 (near NRP2, FUD-associated), rs10908366 (near RSP01, HFU-associated) and rs11940736 (near SPRY1, HFU-associated). Effect sizes (dots) and standard error (bars) are shown for the Taizhou Longitudinal Study (TZL; red) and National Survey of Physical Traits (NSPT; blue) cohorts. chr, chromosome; CI, confidence interval; SNP, single nucleotide polymorphism.

variation in these traits, in agreement with previous findings.²⁴

We performed discovery GWAS for HFU and FUD in the TZL cohort, and found no evidence of genomic inflation [linkage disequilibrium score regression intercept < 1.03, $\lambda < 1.03$; Figure S1 (see Supporting Information)]. For HFU, we identified a novel association at 4q28.1, where 225 single nucleotide polymorphisms (SNPs) in high linkage disequilibrium ($r^2 > 0.5$) met genome-wide significance ($P < 5 \times 10^{-8}$). The leading SNP, rs11940736 ($P = 9.38 \times 10^{-10}$), lies intronic to SPATA5. Replication testing for rs11940736 in the NSPT cohort validated the same direction of effect ($P = 3.23 \times 10^{-3}$). For FUD, the discovery GWAS did not yield any genome-wide significant signals.

We next conducted a meta-analysis that integrated the discovery and replication cohorts (Figure 2, Table 1). For HFU, two loci surpassed the genome-wide significance threshold: one at rs11940736 (P=3.62 \times 10⁻¹¹) replicating the discovery signal, and a novel signal at 1p34.3 marked by rs10908366 (P=4.17 \times 10⁻⁹). For FUD, the meta-analysis uncovered a significant association at 2q23.3, where rs3771033 within the intronic region of *NRP2* attained genome-wide significance (P=4.52 \times 10⁻⁹). Conditional GWAS analysis that controlled these lead SNPs did not reveal further significant loci. Further sex-stratified meta-analysis did not reveal any new loci (Figure S2; see Supporting Information).

4q28.1

The 4q28.1 locus was the only region that met our stringent discovery replication criteria. The lead SNP, rs11940736, consistently influenced HFU in the TZL (β =0.04, P=9.38×10 $^{-10}$) and NSPT (β =0.02, P=3.23×10 $^{-3}$) cohorts, with no effect observed on FUD. Analysis using the 1000GP dataset showed a trend where the derived C allele of rs11940736, associated with higher HFU, decreased in frequency from European populations (0.87) to East Asian populations (0.54), with African populations showing an intermediate frequency (0.66). This allele distribution contrasts with global HFU patterns, where African populations exhibit the highest HFU. Therefore, the 4q28.1 locus does not account for the differences found in HFU.

Within the 4g28.1 region (123.8-124.3 Mbp), 225 SNPs were primarily concentrated around SPATA5. Functional annotation identified that rs302530 (in high linkage disequilibrium with lead SNP rs11940736, r^2 =0.81), which also showed a genome-wide statistically significant association with HFU ($P=6.25\times10^{-9}$), overlaps one of the few open chromatin peaks in this region (Figure 3b). This chromatin peak, unique to SPRY1 expression (a gene adjacent to SPATA5), is supported by single-cell RNA (scRNA) and single-cell ATAC (assay for transposable-accessible chromatin) data.²⁵ Enhancer activity at this peak is shown by skin histone modification tracks, 26,27 and falls within the same topologically associating domain as SPRY1 (Figure 3c).28 Additionally, rs302530 is located at a CTCF (CCCTC-binding factor) transcription factor binding site in skin (Figure 3e). SPRY1 is a protein-coding gene involved in the negative regulation of the fibroblast growth factor (FGF) receptor signalling pathway. Previous studies have reported that knockout of Spry1 and Spry2 in mouse eyelid epithelial cells induces upregulation of FGF expression and activation of the Wnt

Table 1 Summary of the putative causal single nucleotide polymorphisms (SNPs) found in our study

		Raco pair		Roforonco	Altomotivo	Meta	Meta-analysis	121	TZL cohort	NS	SPT cohort		Ţ	requency.		
	Chromosome	position	Lead SNP	allele	allele	β	P-value	β	P-value	β	P-value	TZL	NSPT	EAS	EUR	AFR
FUD	2	206595810	rs3771033	O	⊢	1.16	4.52×10^{-9}	0.97	1.28×10 ⁻⁴	1.39	4.33×10 ⁻⁵	0.36	0.36	0.34	0.35	0.09
HFU	_	38121934	rs10908366	_	O	0.03	4.17×10^{-9}	0.03	8.01×10^{-6}	0.03	1.77×10 ⁻⁴	0.40	0.43	0.42	0.50	0.46
	4	124171702	rs11940736	_	O	0.03	3.62×10^{-11}	0.04	9.38×10^{-10}	0.02	3.23×10^{-3}	0.53	0.52	0.54	0.87	99.0
	4	124165671	rs302530	_	O	0.03	3.76×10^{-10}	0.04	6.25×10^{-9}	0.02	5.10×10^{-3}	0.52	0.51	0.52	0.71	0.48

European; FUD, follicular unit density; HFU, hairs per follicular unit; NSPT, National Survey of Physical Traits; TZL, Taizhou Longitudinal Study. EUR, AFR, African; EAS, East Asian;

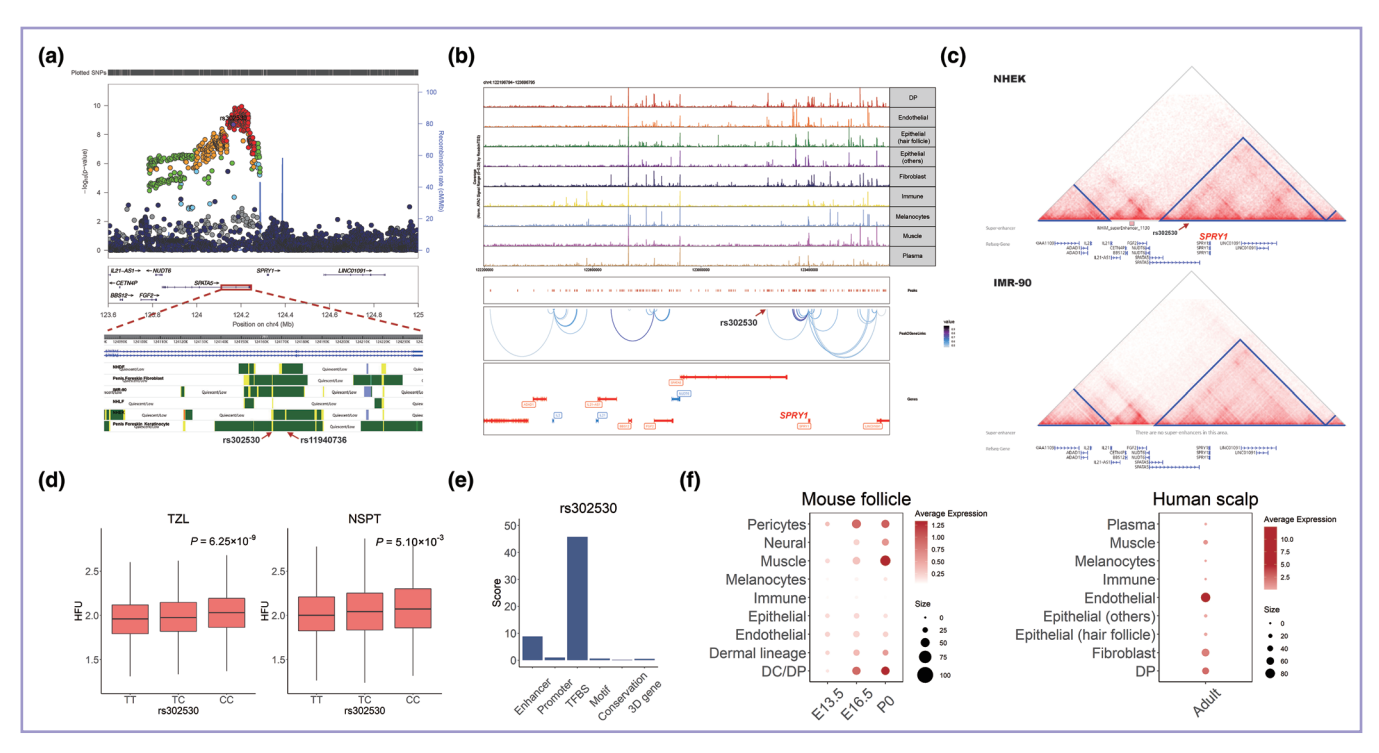


Figure 3 Functional analysis of the 4q28.1 locus associated with hairs per follicular unit (HFU). (a) Regional association plot for the 4q28.1 locus. The lead single nucleotide polymorphism (SNP) rs11940736 and causal SNP rs302530 are highlighted. The zoomed-in view shows histone modification marks of the region. (b) Genome accessibility track visualization of the 4q28.1 locus [chromosome (chr) 4: 122196794-123696795, hg38]. Links represent significant peak-to-gene correlations between the region containing rs302530 and *SPRY1*. (c) Visualization of chromatin interaction by Hi-C data on normal human epidermal keratinocyte (NHEK) and IMR-90 cell lines. (d) Effect of derived alleles of rs302530 shows a contribution to HFU in the Taizhou Longitudinal Study (TZL) and National Survey of Physical Traits (NSPT) cohorts. (e) Functionality scores of rs302530, scored across enhancer, promoter, transcription factor binding site (TFBS) and other regulatory categories. (f) Expression of *SPRY1* in different cell types of mouse dorsal skin and human scalp skin. ATAC, assay for transposable-accessible chromatin; DC, dermal condensate; DP, dermal papilla; NHDF, normal human dermal fibroblast; NHLF, normal human lung fibroblast; TSS, transcription start site.

signalling pathway.²⁹ Similarly, the loss of *Spry1* in mouse mammary fibroblasts leads to upregulation of the ERK pathway, promoting epithelial expansion and migration through paracrine signalling and extracellular matrix remodelling.²⁹ scRNA sequencing (scRNAseq) data have further revealed that (i) *Spry1* expression initiates in the mouse dermal papilla (DP) at E16.5, aligning with the onset of hair follicle development and persisting through the newborn stage;^{25,30,31} and (ii) *SPRY1* is highly expressed in human DP (Figure 3f). Collectively, these findings suggest that rs302530 acts as an enhancer, modulating *SPRY1* expression in the DP.

1p34.3

At the 1p34.3 locus, SNP rs10908366 demonstrated a consistent effect on HFU across the TZL (β =0.03, P=8.01×10⁻⁶) and NSPT (β =0.03, P=1.77×10⁻⁴) cohorts. Analysis of the 1000GP dataset revealed moderate frequency differences for the derived C allele across populations (f_{EAS} =0.42, f_{EUR} =0.50, f_{AFR} =0.46, where EAS denotes East Asian, EUR denotes European and AFR denotes African). SNP rs10908366 is in an intergenic region, 21 kb upstream of RSPO1. Histone modification annotations show that rs10908366 is positioned within a skin-specific enhancer region. According to 3DSNP database annotations, ³² this locus exhibits three-dimensional interactions with the adjacent RSPO1 (Figure S3; see Supporting Information). RSPO1 is an agonist of the Wnt/ β -catenin signalling pathway,

acting as a ligand for LGR4-6 (leucine-rich repeat-containing G-protein coupled receptors) and activating the canonical Wnt signalling pathway. Studies have shown that Rspo1 expression is upregulated before the transition of hair follicles from the telogen to the anagen phase. In vitro experiments have demonstrated that Rspo1 can activate the Wnt/β-catenin signalling pathway, with exogenous R-Spondin1 inducing early entry of mouse hair follicles into the anagen phase.33 Further examination of Rspo1 expression in publicly available scRNAseq data from mouse hair follicles revealed robust expression in the DP. Similarly, scRNAseq data from human scalp show RSPO1 expression specifically within the DP (Figure S3). These findings support our hypothesis that rs10908366 may regulate RSP01 expression via an enhancer mechanism in the DP, potentially influencing HFU by activating the Wnt signalling pathway.

2q23.3

At the 2q23.3 locus, rs3771033 demonstrated a consistent effect on FUD across the TZL (β =0.97, P=1.28×10⁻⁴) and NSPT (β =1.39, P=4.33×10⁻⁵) cohorts. Additionally, this SNP showed a nominally significant association with HFU in the meta-analysis (β =-0.02, P=4.88×10⁻⁵). The derived T allele exhibits a notably lower frequency in African populations (f_{EAS}=0.34, f_{EUR}=0.35, f_{AFR}=0.09), suggesting a potential impact on global hair density variations. Fixation index (F_{ST}) analysis confirmed differentiation

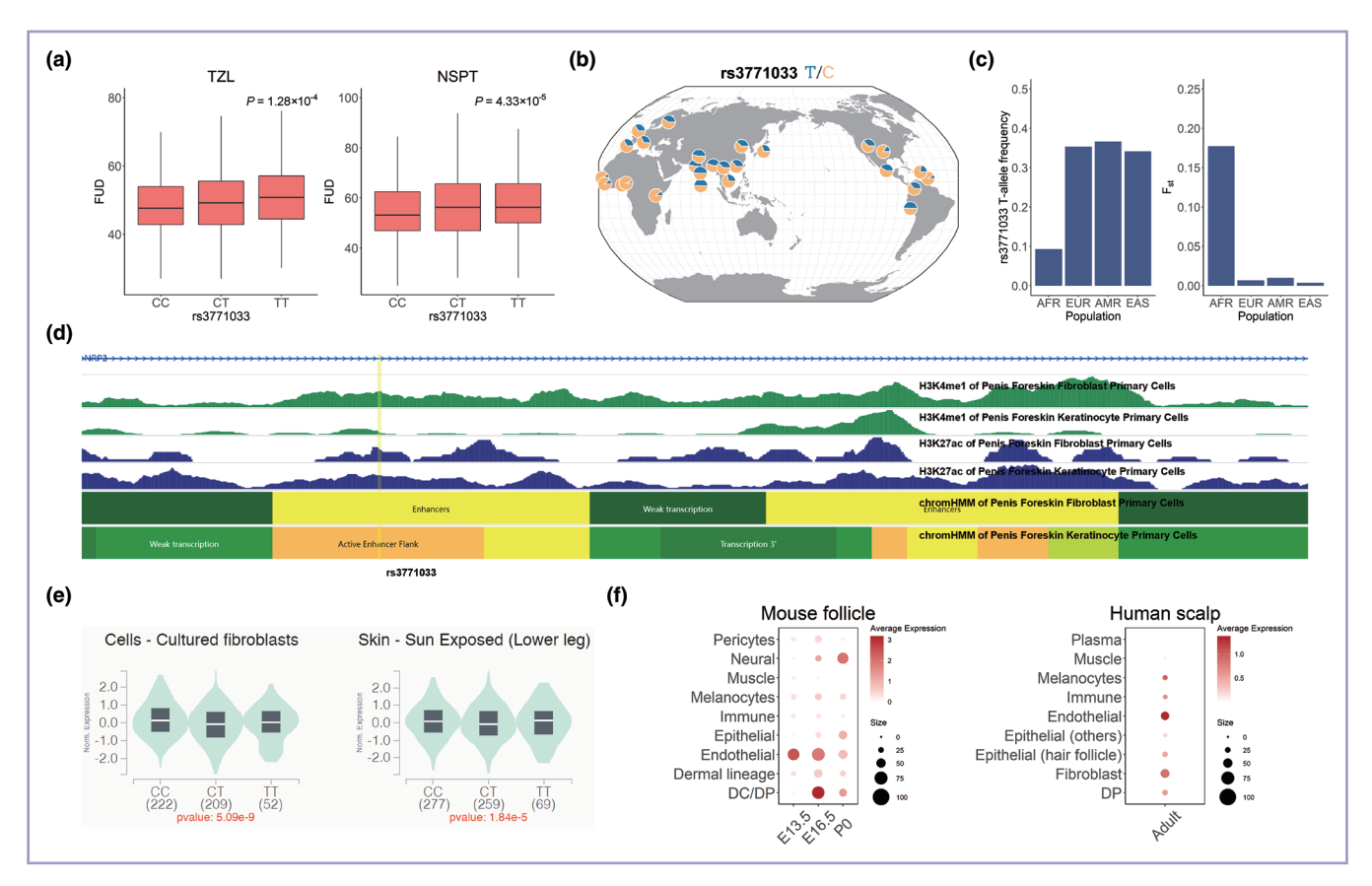


Figure 4 Functional analysis of the 2q23.3 locus associated with follicular unit (FU) density (FUD). (a) Effect of derived alleles of rs3771033 contribute to FUD (FU cm⁻²) in the Taizhou Longitudinal Study (TZL) and National Survey of Physical Traits (NSPT) cohorts. (b) The geography of allele frequency on rs3771033. (c) Bar plot showing the derived allele frequency and fixation index (F_{ST}) value for rs3771033. (d) Visualization of epigenetic tracks H3K4me1 and H3K27ac at the region around rs3771033, annotated by Roadmap. (e) Expression quantitative trait locus analysis by GTEx shows an association between rs3771033 genotypes and the expression of *NRP2* in fibroblasts and sun-exposed skin. (f) Expression of *NRP2* in different mouse dorsal skin and human scalp skin cells. AFR, African; AMR, American; DC, dermal condensate; DP, dermal papilla; EAS, East Asian; EUR, European.

between African populations and others at rs3771033 (F_{ST} =0.18), indicating possible natural selection influences (Figure 4c).

Histone modification tracks from Roadmap (https:// epigenomegateway.wustl.edu/browser/) revealed strong enhancer activity at rs3771033, particularly with H3K4me1 and H3K27ac marks in fibroblasts and keratinocytes (Figure 4d). GTEx data indicated a significant association between rs3771033 and NRP2 expression in skin ($\beta = -0.11$, $P=1.8\times10^{-5}$; Figure 4e), ³⁴ suggesting that the C to T allele shift reduces NRP2 expression. NRP2, a member of the neuropilin family that interacts with vascular endothelial growth factor, is involved in cardiovascular development, axon guidance and tumorigenesis, and is essential for hair follicle morphogenesis by guiding the polarization of dermal condensate precursors into DP.31 scRNAseq data from mouse hair follicles show high Nrp2 expression in dermal condensate at E16.5 (a key hair follicle development stage) with reduced expression in DP at newborn stage (P0). In human scalp single-cell data, NRP2 is also highly expressed in DP (Figure 4f). These findings suggest that rs3771033 may regulate NRP2 expression via an enhancer mechanism, influencing DP development and hair morphogenesis.

Combined genome-wide association studies of hair density, eyebrow thickness, beard thickness and hair curliness

We used C-GWAS to increase statistical power and identify additional loci associated with hair density by leveraging shared genetic factors across multiple hair traits. Specifically, we integrated findings from six previous GWAS on hair-related phenotypes, including eyebrow thickness, beard density and hair curliness, 9-13 encompassing diverse ancestries. Before the C-GWAS, we separately performed meta-analysis on hair curliness and eyebrow thickness (Figure S4; see Supporting Information). 9-13 Our C-GWAS combined the results of these meta-analyses with the GWAS on beard density and our own meta-analysis on FUD and HFU. We excluded the MPB GWAS by Yap et al., 15 owing to its exceptionally large sample size using UK Biobank data, which risked disproportionately amplifying MPB signals.

C-GWAS identified 16 significant loci, including the 3 loci discovered in our meta-analysis. Among these, three additional loci – *PREP* (6q21), *GATA3* (10p14) and *MAF* (16q23.2) – were identified through their association with hair density, reflecting our goal of increasing the power to

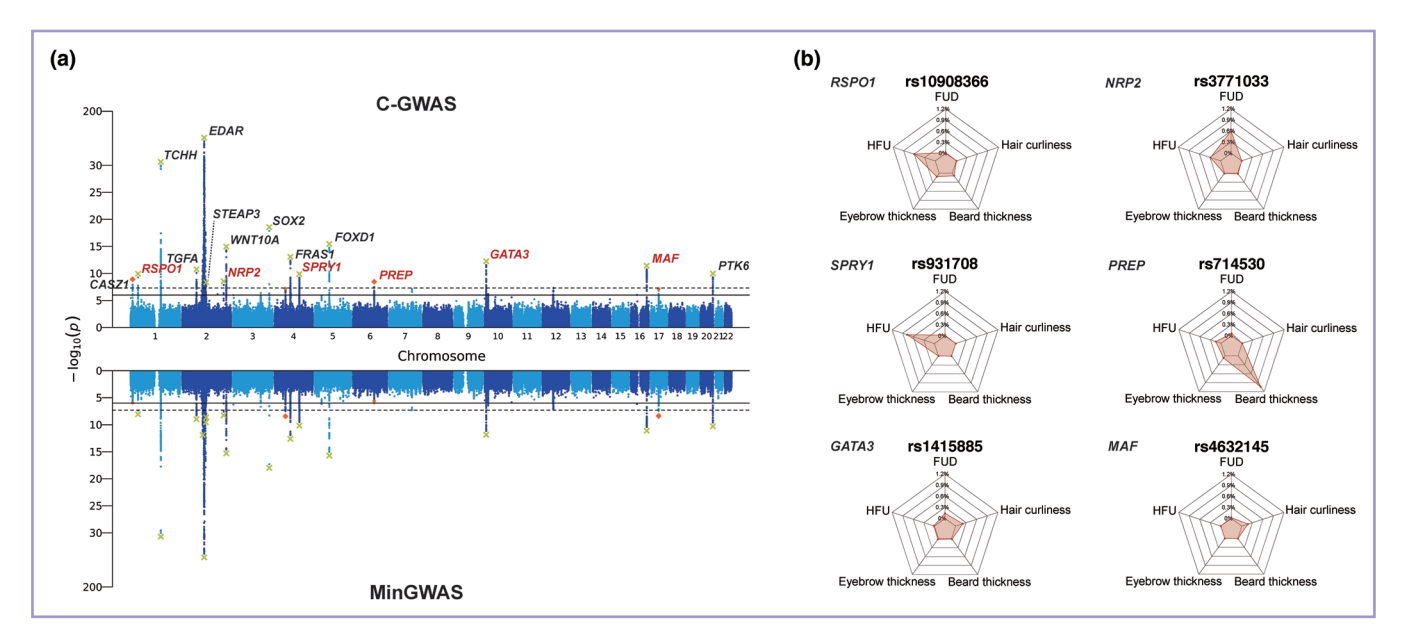


Figure 5 Combined genome-wide association studies (C-GWAS) across hair-related traits identified additional signals. (a) C-GWAS incorporating follicular unit density (FUD), hairs per follicular unit (HFU), meta-analysed results for hair curliness, eyebrow thickness and beard thickness. 9-13 The C-GWAS *P*-values (upper panel) are compared with the lowest *P*-values from individual-trait GWAS (MinGWAS: lower panel) at the –log₁₀ scale. (b) Radar plots illustrating the phenotypic variance explained by single nucleotide polymorphisms, highlighting the multitrait genetic effects.

identify additional hair density-related signals (Figure 5, Table 2). At the 1p34.3 locus near RSPO1 (rs10908366), we found a two-order-of-magnitude increase in significance, driven by HFU ($P=4.17 \times 10^{-9}$) and eyebrow thickness ($P=7.30 \times 10^{-5}$). A similar increase was found at the 6g21 locus near PREP (rs714530), driven by HFU ($P=3.55\times10^{-3}$), eyebrow thickness ($P=6.17 \times 10^{-4}$) and beard thickness ($P=3.98 \times 10^{-7}$). At 10p14 near GATA3 (rs1415885), significant contributions were made by FUD ($P=4.91\times10^{-3}$) and hair curliness $(P=2.04\times10^{-13})$. Finally, the 16g23.2 locus within MAF (rs4632145) showed increased significance based on FUD $(P=6.42\times10^{-3})$ and hair curliness $(P=1.64\times10^{-12})$, marking the first report to date of MAF influencing hair curliness. Collectively, these findings underscore the utility of a multitrait approach to amplifying statistical power, facilitating the discovery of novel loci associated with hair density.

Shared genetic factors between hair density and male pattern baldness

We investigated whether key SNPs identified in studies of MPB by Yap *et al.* also affected our hair density phenotypes (Table S4; see Supporting Information). ¹⁵ Among the 598 reported MPB SNPs, 458 were available in our dataset. Thirty of these were nominally significantly associated with FUD and 39 with HFU (P<0.05), exceeding the expected 5% under the null (binomial test P<1×10⁻⁵). Notably, *RSPO1* and *NRP2* – two loci from our hair density GWAS – achieved genome-wide significance in MPB, suggesting a shared genetic architecture.

In a subset of the NSPT cohort, we explored the relationship between hair density and hair loss severity and found that hair loss had a minimal impact on hair density-associated signals (Appendix S1, Figure S5; see Supporting Information), suggesting that the overlap between hair density and MPB loci is unlikely to be driven by hair loss.

A phenome-wide association study in the GWAS Atlas (4756 phenotypes; https://atlas.ctglab.nl/) and Biobank Japan (230 phenotypes; https://biobankjp.org/en/) revealed no additional significant associations outside MPB for our hair density SNPs [Figure 6a; Figure S6, Table S5 (see Supporting Information)].

Gene-hormone and finasteride interactions in hair density

In a combined sample of 3669 women from the NSPT and TZL cohorts, we evaluated 3 SNPs identified by our GWAS for hair density and tested their interactions with 6 hormone-related factors (Table S6; see Supporting Information). Nominal significance emerged for rs3771033 in interaction with age at menopause ($P=8.44\times10^{-3}$) and age at first pregnancy ($P=2.33\times10^{-2}$), whereby women carrying the T allele who had a later menopause or a later first pregnancy showed higher FUD. Noncarriers did not exhibit these trends. Considering that rs3771033 is also associated with MPB, we were prompted to investigate whether it interacts with finasteride, a hormone-related treatment for MPB. To explore this hypothesis, we leveraged treatment record data from the UK Biobank to assess genotype-specific effects on finasteride efficacy. A significant gene-treatment interaction $(P=2.6\times10^{-3})$ indicated that T-allele carriers had a notably better finasteride response than noncarriers at baseline, as well as after approximately 13 years of follow-up (Figure 6b). In contrast, rs10908366 (P=0.71) and rs302530 (P=0.25) did not exhibit a significant genotype-specific response to finasteride. We then extended the same analysis to an additional set of 598 SNPs reported by Yap et al. as MPB risk variants and discovered that 1 SNP (rs12737859; $P=3.64\times10^{-6}$) [Figure 6c; Table S7 (see Supporting Information)]¹⁵ survived multiple testing of 598 independent tests, which demonstrated an even stronger interaction effect than rs3771033.

														2		2	3	calliless	1	The second	5	Deal a cilicaliess
													Eas	East Asian	Eas	East Asian	East Asia Latin /	East Asian, European, Latin American	East Asia Latin	East Asian, European, Latin American	Latin A	Latin American
							ш	Frequency	>				meta (n=	Our meta-analysis (n=5735)	Our me	Our meta-analysis (n=5735)	Meta-ana Liu anc $(n=2)$	Meta-analyses of Wu, Liu and Adhikari $(n=23.293)^{9-11}$	Meta-an an $(n=1)$	Meta-analyses of Wu and Peng $(n=15.931)^{12.13}$	GW Adi	GWAS of Adhikari (n=2922) ¹¹
Band	Nearest gene	SNP	Base pair position	Reference allele	Reference Altemative allele allele	EAS	EUR	AFR	AMR	SAS	C-GWAS P-value ^a	MinGWAS P-value ^b	6	P-value	В	P-value	Z-value	P-value	Z-value	P-value	В	P-value
1p36.22	CIROZ; CASZ1	rs12081181	11034165	F	ŋ	0.19	0.23	0.70	0.27	0.18	1.13×10 ⁻⁸	1.16×10-6	SN	SN	SN	SN	SN	NS	-4.10	4.07×10 ⁻⁵	-0.14	1.86×10 ⁻⁷
1p34.3 1q21.3	RSPO1 TCHH;	rs10908366 rs2999559	38121934 151997199	⊢∢	υυ	0.42	0.50	0.46	0.44	0.27	5.58× 10 ⁻¹⁰ 1.11× 10 ⁻³⁰	4.27× 10 ⁻⁸ 5.09× 10 ⁻³¹	SZZ	S SN	0.03 NS	4.17x 10 ⁻⁹ NS	NS -12.15	NS 5.85×10 ⁻³⁴	3.97 NS	7.30 × 10 ⁻⁵ NS	S S	S S S
2p.13 3	1 ST	re7605323	70283607	F	ر	0.37	000	0.07	0.37	0.25	17 ~ 10-11	E 27 ~ 10-9	V	<u>V</u>	O N	<u>U</u>	6 37	2 55 > 10-10	N	ON N	010	2 66 > 10-4
2912.3	FDAR	rs3827760	109513601	- ∢) (C	0.87	0.01	0.00	0.39	, , ,	7.73×10^{-144}	5.21×10 ⁻¹²⁶	2 2	2 S	2 2	o s S	-24.83	4.79×10 ⁻¹³⁶	22.50	6.82×10-9	0.22	1.15×10 ⁻¹⁶
2q14.2	STEAP3	rs113989113	119966031	1	-	0.08	0.41	0.14	0.27		2.12×10-8	1.11×10-8	NS	NS	NS	SN	6.20	5.64×10 ⁻¹⁰	ı	1	NS	SN
2q33.3	NRP2	rs3771033	206595810	O	-	0.34	0.35	0.09	0.37		1.32×10 ⁻⁸	2.70×10^{-8}	1.16	4.52×10^{-9}	-0.02	4.88×10 ⁻⁵	NS	NS	NS	NS	NS	NS
2q35	WNT10A	rs74333950	219746292	⊢	g	0.24	0.12	0.23	0.13		5.05×10^{-15}	2.47×10^{-15}	SN	NS	NS	NS	8.41	4.11×10^{-17}	NS	NS	NS	NS
3q26.33	SOX2-OT; SOX2	rs1345417	181511951	O	O	0.29	0.63	99.0	0.52	0.63	1.33× 10 ⁻¹⁸	4.96×10 ⁻¹⁸	SN	SN	SN	SN	NS	NS	9.01	2.06×10^{-19}	0.09	6.09×10 ⁻⁴
4q21.21	FRAS1	rs440095	79279801	∢	g	0.26	99.0	09.0	0.65	0.43	4.17×10^{-13}	1.23×10^{-12}	SN	NS	NS	NS	-7.59	3.21×10^{-14}	NS	NS	0.07	3.81×10 ⁻³
4q28.1	SPATA5;	rs931708	124202363	U	∢	0.54	0.83	0.36	0.78	09.0	6.16×10^{-10}	3.15×10^{-10}	SN	NS	0.03	2.51×10^{-11}	NS	NS	NS	NS	NS	NS
5013.2	FOXD 1	re6881396	72559339	F	ď	0.14	0.41	0 59	0.32	0 20	168 > 10-15	9 30 > 10-16	V	SN	V	S	V	SN	8	4 75 > 10-17	-0.05	4 15 × 10-2
6q.13.2	PREP	rs714530	106042885	- U) ⊢	0.16	0.46	0.04	0.37		3.19×10-8	2.45×10-6	SZ	S Z	0.02	3.55×10-3	S S	SZ	3.42	6.17×10⁴	0.13	3.98×10-7
10p14	GATA3	rs1415885	8352561	O	-	0.79	0.64	0.60	69.0		2.74×10^{-12}	6.87×10^{-12}	-0.67	4.91×10 ⁻³	NS	NS	-7.35	2.04×10^{-13}	NS	NS	NS	NS
16q23.2	MAF	rs4632145	79797279	ŋ	O	0.24	0.16	0.38	0.20	0.26	1.84×10^{-11}	4.78×10 ⁻¹¹	-0.64	6.42×10^{-3}	NS	NS	2.06	1.64×10^{-12}	SN	NS	NS	NS
20q13.33	PTK6	rs310644	62159504	—	O	0.04	0.07	0.91	0.13	0.41	4.97×10^{-10}	2.54×10^{-10}	SN	NS	NS	SN	6.81	9.82×10^{-12}	NS	SN	NS	NS

Table 2 Summary of the combined genome-wide association studies (C-GWAS) result

South Asian; (-), onal lead single nucleotide polymorphism (SNP) is displayed. AFR, African, AMR, American, EAS, East Asian; EUR, European, FUD, follicular unit density; HFU, hairs per follicular unit; NS, not significant (P>0.05); SAS, Sout after exempte the P-value obtained by combining multiple GWAS of correlated traits. Bepresents the minimum P-value from individual-trait GWAS analyses, adjusted through simulations embedded in the C-GWAS software. Notably, rs12737859 lies in an intron of *ECE1*, a gene that processes endothelin and regulates vascular tone and tissue homeostasis. In parallel, rs3771033 resides within *NRP2*, which encodes a co-receptor for vascular endothelial growth factor, which modulates local blood flow and angiogenesis. *ECE1* and *NRP2* thus appear to be integral to maintaining a supportive vascular and microenvironmental milieu for hair follicles, especially under the reduced dihydrotestosterone conditions induced by finasteride. These findings highlight a potentially critical role for genotype-specific modulation of vascular and endothelin pathways in hair development and underscore the utility of targeted pharmacogenomic approaches.

Discussion

In our study of 5735 East Asian individuals, significant influences on hair density traits were identified from age, sex, BMI, age of menarche, age at first pregnancy and menopause status, with age negatively correlating with both FUD and HFU. Our GWAS pinpointed three loci that affect hair density: rs11940736 at 4g28.1 near SPRY1 affecting HFU; rs10908366 at 1p34.3 near RSPO1 also impacting HFU; and rs3771033 at 2g23.3 within NRP2 influencing FUD. The significance of rs11940736 was validated in an independent cohort. These loci modulate hair traits by regulating genes critical for hair follicle development and morphogenesis. C-GWAS analysis identified additional loci relevant to hair density, demonstrating the power of leveraging shared genetic factors across multiple hair-related phenotypes. Notably, shared genetic signals with MPB and other hair-related traits point to overlapping biologic mechanisms, suggesting that interventions targeting these pathways may yield multifaceted therapeutic benefits. Our data indicated that genotype-specific responses to finasteride (e.g. at NRP2 and ECE1) modulate vascular support within the follicular microenvironment, hinting at the high potential for pharmacogenomics in hair loss treatment.

For phenotype quantification, we used deep learning models, subsequently manually correcting the data due to limitations in accuracy. 11,36 We analysed the occipital scalp, which is less affected by androgen-induced hair loss, 16,17 although men still showed a higher FUD, indicating potential androgenic effects. Despite there being no significant findings near the androgen receptor gene, 37,38 our results emphasize the role of multiple genetic and hormonal pathways in hair density.

Our findings underscore the complexity of the genetic regulation of hair biology, involving the Wnt signalling pathway and others.^{39–41} Although the identified SNPs explain only a portion of the heritability, they offer insights into the molecular mechanisms affecting HFU and FUD. Environmental factors and gene–environment interactions are also likely to contribute, as indicated by higher genetic vs. phenotypic correlations.

Given that our GWAS cohorts consisted exclusively of East Asian individuals, the generalizability of our findings to broader populations is limited, warranting future association and functional studies in different populations. Understanding these mechanisms may lead to targeted treatments for hair growth disorders and enhance

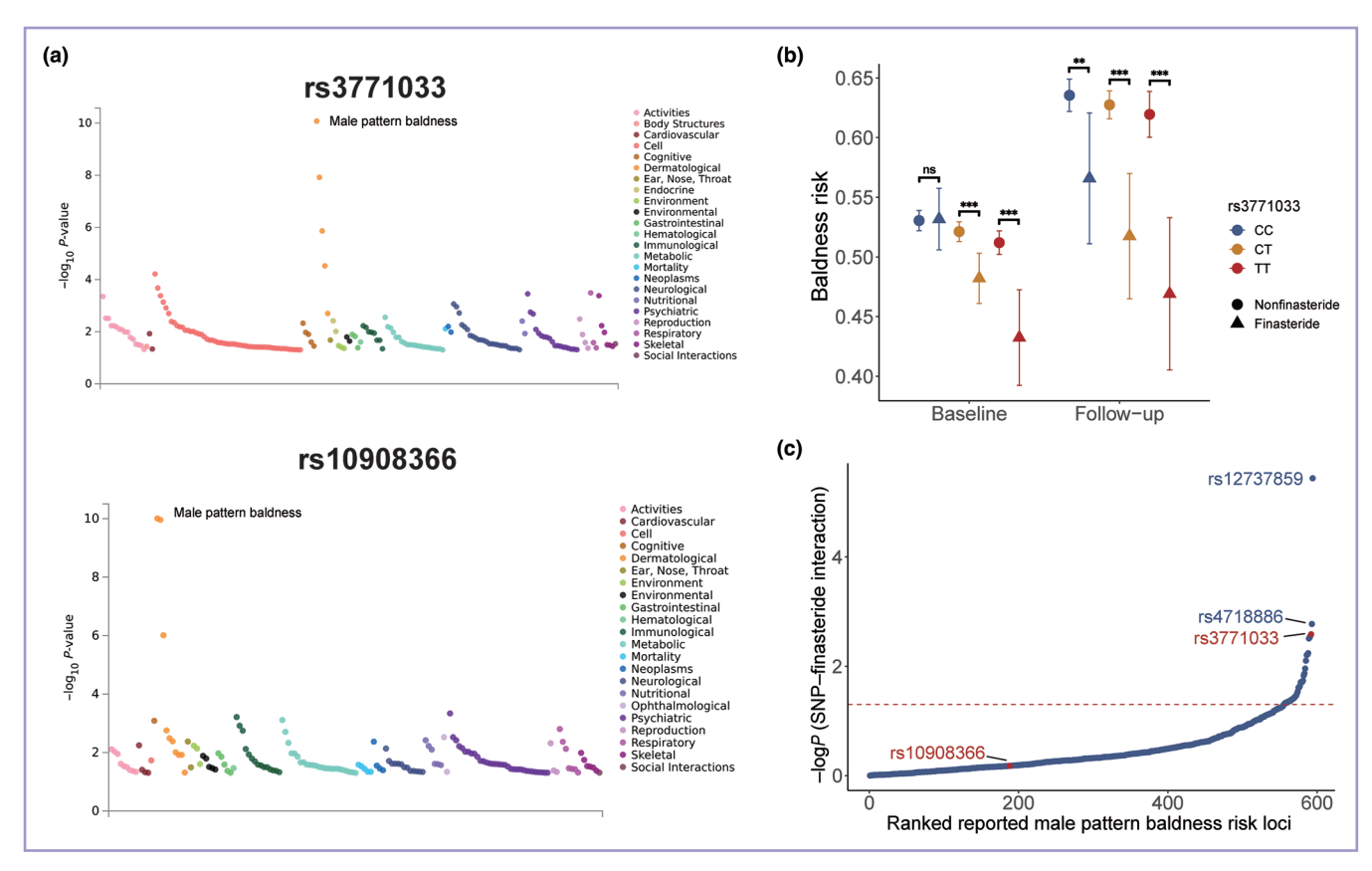


Figure 6 Single nucleotide polymorphism (SNP)–finasteride interactions affecting male pattern baldness. (a) Phenome-wide association study of hair density-related SNPs in the GWAS Atlas (https://atlas.ctglab.nl/). (b) Longitudinal analyses of UK Biobank data on risk of baldness, stratified by the genotype of rs3771033 and finasteride use. (c) Finasteride interaction scan for 598 known risk SNPs reported by Yap *et al.* and rs3771033.¹⁵ The y-axis shows $-\log_{10}(P)$ for SNP–finasteride interactions in the mixed linear model. ns, not significant (P>0.05). **P<0.01, ***P<0.001.

personalized medicine in dermatology. Our GWAS also identifies potential targets like *SPRY1*, *RSPO1* and *NRP2* for the development of treatments for hair disorders, with implications for managing conditions like hair loss across multiple related disorders.

Acknowledgements

We thank the volunteers in the Taizhou Longitudinal Study cohort and the National Survey of Physical Traits cohorts for their enthusiastic support of this research. We thank the Human Phenome Data Center of Fudan University for the invaluable support. We thank the participants of the UK Biobank study for enabling us to conduct this research. Some graphical illustrations in this manuscript were generated using Biorender.com.

Funding sources

This work was supported by National Key R&D Program of China (2024YFC3405800 to S. Wang), the Strategic Priority Research Program of the Chinese Academy of Sciences (CAS; XDB38020400 to S. Wang), CAS Young Team Program for Stable Support of Basic Research (YSBR-077 to S. Wang), CAS Interdisciplinary Innovation Team to S. Wang, CAS Youth Innovation Promotion Association (2020276 to Q. Peng), Shanghai Municipal Science and Technology

Major Project (2017SHZDZX01 to S. Wang, L. Jin, J. Wang and Q. Peng), Shanghai Science and Technology Innovation Action Project (24JS2810300 to S. Wang), the National Natural Science Foundation of China (32325013 and 92249302 to S. Wang; 32471216 to Q. Peng), the National Key Research and Development Project (2018YFC0910403 to S. Wang), Ministry of Science and Technology of the People's Republic of China (2015FY111700 to L. Jin), Shanghai Science and Technology Commission Excellent Academic Leaders Program (22XD1424700 to S. Wang), 111 Project (B13016 to L. Jin), CAMS Innovation Fund for Medical Science (2019-I2M-5-066 to J. Wang and L. Jin) and Naif Arab University for Security Sciences (NAUSS-23-R18, NAUSS-23-R19 to F. Liu).

Conflicts of interest

The authors declare no conflicts of interest.

Data availability

The genome-wide association study summary statistics are available for download from the Genome Variation Map of the National Genomics Data Center, Beijing Institute of Genomics, Chinese Academy of Sciences and China National Center for Bioinformation under accession number GVP000050.^{42,43} Data use must be in full compliance

with the Regulations on Management of Human Genetic Resources in China. Individual genotype and phenotype data cannot be shared owing to Institutional Review Board restrictions on privacy concerns. Data from the UK Biobank were used under license and are thus not publicly available but can be accessed through their standard application process (https://www.ukbiobank.ac.uk/register-apply/). Data used in this study are available in the UK Biobank under application number 77803. Other relevant data supporting the key findings of this study are available in the article and its Supporting Information or on reasonable request from the corresponding author.

Ethics statement

Ethical approval for the Taizhou Longitudinal Study was obtained from the ethics committee of Fudan University, Shanghai, China (Ethics Research Approval 85). Ethical approval for the National Survey of Physical Traits was granted by the Shanghai Institutes for Biological Sciences (ER-SIBS-261410).

Patient consent

All participants in the Taizhou Longitudinal Study and National Survey of Physical Traits provided written informed consent.

Supporting Information

Additional Supporting Information may be found in the online version of this article at the publisher's website.

References

- 1 Loussouarn G, El Rawadi C, Genain G. Diversity of hair growth profiles. Int J Dermatol 2005; 44(Suppl. 1):6–9.
- 2 Lee HJ, Ha SJ, Lee JH et al. Hair counts from scalp biopsy specimens in Asians. J Am Acad Dermatol 2002; 46:218–21.
- 3 Ko JH, Huang YH, Kuo TT. Hair counts from normal scalp biopsy in Taiwan. *Dermatol Surg* 2012; **38**:1516–20.
- 4 Bernstein RM, Rassman WR. Follicular transplantation. Patient evaluation and surgical planning. *Dermatol Surg* 1997; 23:771–84.
- 5 Visessiri Y, Pakornphadungsit K, Leerunyakul K et al. The study of hair follicle counts from scalp histopathology in the Thai population. Int J Dermatol 2020; 59:978–81.
- 6 Devjani S, Ezemma O, Kelley KJ *et al.* Androgenetic alopecia: therapy update. *Drugs* 2023; **83**:701–15.
- 7 Almohanna HM, Ahmed AA, Tsatalis JP et al. The role of vitamins and minerals in hair loss: a review. *Dermatol Ther (Heidelb)* 2019; 9:51–70.
- 8 Hasan R, Juma H, Eid FA et al. Effects of hormones and endocrine disorders on hair growth. Cureus 2022; **14**:e32726.
- 9 Wu S, Tan J, Yang Y et al. Genome-wide scans reveal variants at EDAR predominantly affecting hair straightness in Han Chinese and Uyghur populations. Hum Genet 2016; 135:1279–86.
- 10 Liu F, Chen Y, Zhu G et al. Meta-analysis of genome-wide association studies identifies 8 novel loci involved in shape variation of human head hair. Hum Mol Genet 2018; 27:559–75.
- 11 Adhikari K, Fontanil T, Cal S et al. A genome-wide association scan in admixed Latin Americans identifies loci influencing facial and scalp hair features. Nat Commun 2016; 7:10815.
- 12 Wu S, Zhang M, Yang X et al. Genome-wide association studies and CRISPR/Cas9-mediated gene editing identify regulatory

- variants influencing eyebrow thickness in humans. *PLoS Genet* 2018; **14**:e1007640.
- 13 Peng F, Xiong Z, Zhu G *et al.* GWAs identify DNA variants influencing eyebrow thickness variation in Europeans and across continental populations. *J Invest Dermatol* 2023: **143**:1317–22.
- 14 Pirastu N, Joshi PK, de Vries PS et al. GWAS for male-pattern baldness identifies 71 susceptibility loci explaining 38% of the risk. Nat Commun 2017; 8:1584.
- 15 Yap CX, Sidorenko J, Wu Y et al. Dissection of genetic variation and evidence for pleiotropy in male pattern baldness. Nat Commun 2018; 9:5407.
- 16 Wirya CT, Wu W, Wu K. Classification of male-pattern hair loss. Int J Trichology 2017; 9:95–100.
- 17 Itami S, Sonoda T, Kurata S *et al.* Mechanism of action of androgen in hair follicles. *J Dermatol Sci* 1994; **7**(Suppl.):S98–103.
- 18 Wang X, Lu M, Qian J et al. Rationales, design and recruitment of the Taizhou Longitudinal Study. BMC Public Health 2009; 9:223.
- 19 Peng Q, Liu X, Li W *et al.* Analysis of blood methylation quantitative trait loci in East Asians reveals ancestry-specific impacts on complex traits. *Nat Genet* 2024; **56**:846–60.
- 20 Yang C-C, Hsieh F-N, Lin L-Y et al. Higher body mass index is associated with greater severity of alopecia in men with male-pattern androgenetic alopecia in Taiwan: a cross-sectional study. J Am Acad Dermatol 2014; 70:297–302.
- 21 Conrad F, Ohnemus U, Bodo E *et al.* Estrogens and human scalp hair growth-still more questions than answers. *J Invest Dermatol* 2004; **122**:840–2.
- 22 Zouboulis CC, Blume-Peytavi U, Kosmadaki M et al. Skin, hair and beyond: the impact of menopause. Climacteric 2022; 25:434–42.
- 23 Fujimoto A, Kimura R, Ohashi J *et al.* A scan for genetic determinants of human hair morphology: EDAR is associated with Asian hair thickness. *Hum Mol Genet* 2008; **17**:835–43.
- 24 Pośpiech E, Karlowska-Pik J, Kukla-Bartoszek M et al. Overlapping association signals in the genetics of hair-related phenotypes in humans and their relevance to predictive DNA analysis. Forensic Sci Int Genet 2022; 59:102693.
- 25 Ober-Reynolds B, Wang C, Ko JM *et al.* Integrated single-cell chromatin and transcriptomic analyses of human scalp identify gene-regulatory programs and critical cell types for hair and skin diseases. *Nat Genet* 2023; **55**:1288–300.
- 26 Kundaje A, Meuleman W, Ernst J *et al.* Integrative analysis of 111 reference human epigenomes. *Nature* 2015; **518**:317–30.
- 27 Birney E, Stamatoyannopoulos JA, Dutta A et al. Identification and analysis of functional elements in 1% of the human genome by the ENCODE pilot project. Nature 2007; 447:799–816.
- 28 Yang D, Jang I, Choi J *et al.* 3DIV: a 3D-genome interaction viewer and database. *Nucleic Acids Res* 2018; **46**:D52–7.
- 29 Koledova Z, Zhang X, Streuli C et al. SPRY1 regulates mammary epithelial morphogenesis by modulating EGFR-dependent stromal paracrine signaling and ECM remodeling. Proc Natl Acad Sci U S A 2016; 113:E5731–40.
- 30 Ge W, Tan S-J, Wang S-H *et al.* Single-cell transcriptome profiling reveals dermal and epithelial cell fate decisions during embryonic hair follicle development. *Theranostics* 2020; **10**:7581–98.
- 31 Saxena N, Mok K-W, Rendl M. An updated classification of hair follicle morphogenesis. *Exp Dermatol* 2019; **28**:332–44.
- 32 Lu Y, Quan C, Chen H *et al.* 3DSNP: a database for linking human noncoding SNPs to their three-dimensional interacting genes. *Nucleic Acids Res* 2017; **45**:D643–9.
- 33 Li N, Liu S, Zhang H-S et al. Exogenous R-Spondin1 induces precocious telogen-to-anagen transition in mouse hair follicles. Int J Mol Sci 2016; 17:582.
- 34 Consortium G. The Genotype-Tissue Expression (GTEx) project. *Nat Genet* 2013; **45**:580–5.
- 35 Xiong Z, Gao X, Chen Y *et al.* Combining genome-wide association studies highlight novel loci involved in human facial variation. *Nat Commun* 2022; **13**:7832.

- 36 Lv W, Chen T, Zeng Y et al. A challenge of deep-learning-based object detection for hair follicle dataset. J Cosmet Dermatol 2023; 22:2565–78.
- 37 Hillmer AM, Hanneken S, Ritzmann S *et al.* Genetic variation in the human androgen receptor gene is the major determinant of common early-onset androgenetic alopecia. *Am J Hum Genet* 2005; **77**:140–8.
- 38 Ellis JA, Stebbing M, Harrap SB. Polymorphism of the androgen receptor gene is associated with male pattern baldness. *J Invest Dermatol* 2001; **116**:452–5.
- 39 Andl T, Reddy ST, Gaddapara T *et al.* WNT signals are required for the initiation of hair follicle development. *Dev Cell* 2002; **2**:643–53.
- 40 Myung PS, Takeo M, Ito M *et al.* Epithelial Wnt ligand secretion is required for adult hair follicle growth and regeneration. *J Invest Dermatol* 2013; **133**:31–41.
- 41 Choi BY. Targeting Wnt/β-catenin pathway for developing therapies for hair loss. *Int J Mol Sci* 2020; **21**:4915.
- 42 Li C, Tian D, Tang B *et al.* Genome Variation Map: a worldwide collection of genome variations across multiple species. *Nucleic Acids Res* 2021; **49**:D1186–91.
- 43 CNCB-NGDC Members and Partners. Database Resources of the National Genomics Data Center, China National Center for Bioinformation in 2022. *Nucleic Acids Res* 2022; **50**: D27–38.